nature ecology & evolution

ARTICLES

https://doi.org/10.1038/s41559-020-1186-6

Check for updates

A competing-risks model explains hierarchical spatial coupling of measles epidemics en route to national elimination

Max S. Y. Lau[1,6]✉, Alexander D. Becker[2,6], Hannah M. Korevaar[2], Quentin Caudron[2], Darren J. Shaw[3], C. Jessica E. Metcalf[2], Ottar N. Bjørnstad[4] and Bryan T. Grenfell[2,5]

Apart from its global health importance, measles is a paradigm for the low-dimensional mechanistic understanding of local nonlinear population interactions. A central question for spatio-temporal dynamics is the relative roles of hierarchical spread from large cities to small towns and metapopulation transmission among local small population clusters in measles persistence. Quantifying this balance is critical to planning the regional elimination and global eradication of measles. Yet, current gravity models do not allow a formal comparison of hierarchical versus metapopulation spread. We address this gap with a competing-risks framework, capturing the relative importance of competing sources of reintroductions of infection. We apply the method to the uniquely spatio-temporally detailed urban incidence dataset for measles in England and Wales, from 1944 to the infection's vaccine-induced nadir in the 1990s. We find that despite the regional influence of a few large cities (for example, London and Liverpool), metapopulation aggregation in neighbouring towns and cities played an important role in driving national dynamics in the prevaccination era. As vaccination levels increased in the 1970s and 1980s, the signature of spatially predictable spread diminished: increasingly, infection was introduced from unidentifiable random sources possibly outside regional metapopulations. The resulting erratic dynamics highlight the challenges of identifying shifting sources of infection and characterizing patterns of incidence in times of high vaccination coverage. More broadly, the underlying incidence and demographic data, accompanying this paper, will also provide an important resource for exploring nonlinear spatiotemporal population dynamics.

The widespread use of an effective vaccine since the mid-1960s has greatly reduced the global circulation of measles. However, the virus continues to be a major cause of death among young children in sub-Saharan Africa[1,2]. Even in many countries with previously effective control, the recent re-emergence of measles, often fuelled by vaccine hesitancy, further confirms measles as an important public health problem globally[3,4]. A simple natural history of infection, and reliable and detailed case notification across an array of settings[5,6], also make measles one of the best-documented spatio-temporal disease systems, in particular, and ecological consumer-resource model systems more generally[7,8]. However, substantial gaps still exist in our understanding of measles spread; we address these lacunae here.

Measles dynamics before and since the introduction of mass vaccination are particularly richly documented by historical notifications in England and Wales (E&W) (Supplementary Figs. 1 and 2 and data in Supplementary Note 1). Before widespread vaccination, measles epidemics in E&W (and many developed countries) were characterized by highly seasonal periodic (often biennial) cycles in large cities and erratic outbreaks driven by extinction–recolonization processes in smaller places (Supplementary Fig. 1a)[5,9]. The critical community size (CCS) of about 300,000 people for measles in prevaccination E&W is the empirically identified threshold required for sustained local chains of infection[10]. In 1960, roughly 16% of the population of E&W inhabited ten big cities above the CCS. Previous studies have identified these cities as the pacemakers for regional dynamics[5,9]. The remaining 84% of the population were subdivided among more than 1,000 smaller conurbations and rural areas, with more irregular dynamics. Since its introduction in 1968, vaccination has substantially reduced the magnitude and regularity of epidemics throughout the regional hierarchy[11] (Supplementary Fig. 1a). This trend is accompanied by a decline in local persistence (Supplementary Fig. 1b), which was especially marked as vaccination rates increased in the 1980s and regional dynamics became increasingly decorrelated[5,11].

At the scale of the metapopulation (here, defined by cities and towns), measles persistence depends on the reintroduction of infection following extinction in local small communities. Previous work has stressed the role of hierarchical core–satellite spread from large to small conurbations in the prevaccination era (Fig. 1a), as a particularly clear exemplar of forest-fire-like extinction–recolonization dynamics[12,13]. This hypothesis is supported by a wavelet phase analysis, which reveals spatial waves travelling from core cities (in particular, London and the industrial north-west) to smaller, more peripheral satellite towns and villages[5]. However, a deeper understanding of how and to what extent these large cities and other competitor infective sources drive the overall disease dynamics is still lacking, particularly as regards the role of the local

[1]Department of Biostatistics and Bioinformatics, Rollins School of Public Health, Emory University, Atlanta, GA, USA. [2]Department of Ecology and Evolutionary Biology, Princeton University, Princeton, NJ, USA. [3]Royal (Dick) School of Veterinary Studies & The Roslin Institute, University of Edinburgh, Midlothian, UK. [4]Center for Infectious Disease Dynamics, Department of Biology, Pennsylvania State University, University Park, PA, USA. [5]Fogarty International Center, National Institutes of Health, Bethesda, MD, USA. [6]These authors contributed equally: Max S. Y. Lau, Alexander D. Becker. ✉e-mail: msy.lau@emory.edu

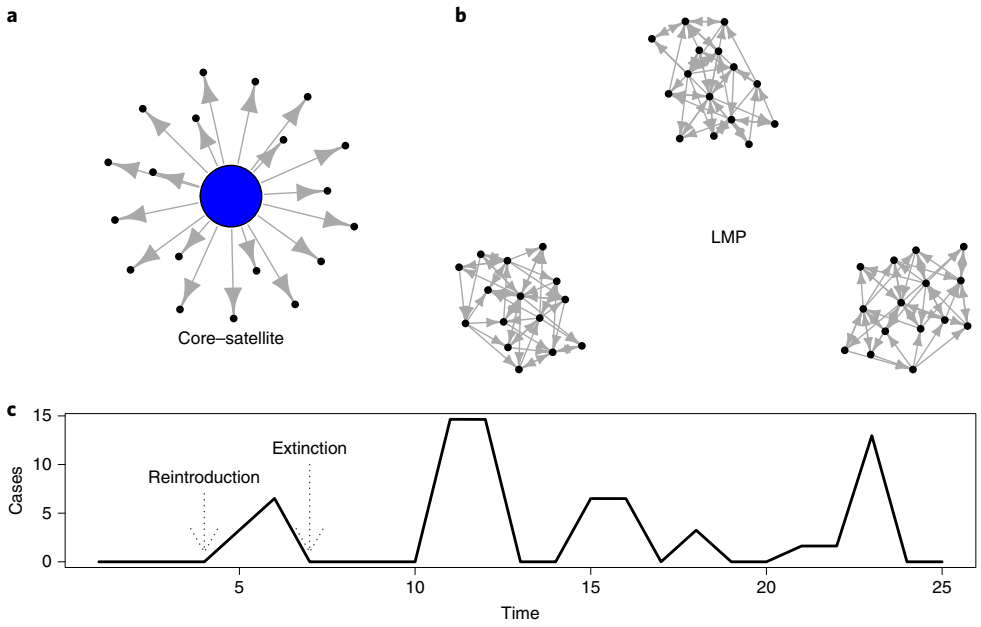

Fig. 1 | A schematic illustration of the spatial dynamics and persistence of measles. a, Core–satellite spread of measles. This represents a hierarchical spread of infection from a core city above the CCS to its nearby smaller towns and villages. **b**, Persistence of measles owing to the local aggregation of communities below the CCS in regional metapopulations (LMP). The core–satellite spread is effectively directional because back-spill does not affect core dynamics, while metapopulation spread is potentially bidirectional. **c**, Schematic illustration of the extinction–recurrent epidemic pattern typically observed in a small town or city. A reintroduction/recolonization time is the time a local epidemic is initiated, and an extinction time is when an epidemic ends in a local fade-out. Unit of time is arbitrary here due to the schematic nature of this illustration.

aggregation of communities below the CCS in regional metapopulations, a mechanism hereafter referred to as local metapopulation persistence (LMP) (Fig. 1b).

The central challenge is to model spatial coupling in a more general sense, to quantify metapopulation synchrony across variable vaccination rates. Inspired by transportation theory[14], Murray and Cliff[15] first proposed that such interactions may be captured by gravity models. This formulation assumes that movement among locales decays with distance but increases in a generalized, bilinear fashion with donor and recipient population sizes. Gravity models and their extensions have provided useful insights into the spatial interactions of many human and non-human disease systems and facilitated disease predictions and explorations of control[9,16,17]. However, in the absence of independent covariates describing human movement (a particularly thorny issue for childhood infections like measles, as historical movement data on children are sparse), model inference—in particular, the simultaneous inference of epidemic trajectories and spatial coupling—is notoriously difficult; researchers have thus resorted to less interpretable non-mechanistic approaches (for example, performing approximations using Gaussian processes)[9,18,19]. While they capture a partial picture of measles dynamics, these methods do not allow for a direct quantification of spatial coupling and systematic titration of the relative importance of different sources of reintroduction of infection. We address this gap by formulating a semimechanistic absence–presence–absence model in a competing-risks framework that focuses explicitly on modelling the reintroduction of infections that are characteristic of small populations (Methods and Fig. 1c). Our approach enables a direct quantification of spatial coupling and allows us to further titrate the relative importance of different sources (for example, LMP versus core–satellite) of reintroduction (that is, a competing-risks framework[20]).

We use this model in tandem with the exhaustive dataset of measles incidence across E&W to dissect and quantify the importance of competing sources of reintroductions of infection in the prevaccination era. We further identify the changing roles of regional gravity coupling and geographically erratic dynamics in seeding epidemics as mass vaccination was rolled out from the late 1960s onwards.

Results

Regional dynamics before vaccination. Prevaccination epidemics in cities above the CCS were largely self-sustaining and insensitive to transient imported infections due to spatial coupling[9,21]; also, extinctions and reintroductions in these larger populations are by definition uncommon. To quantify spatial coupling, we therefore focus our analysis on the timings of epidemics in all populations well below the CCS (872 places with populations less than 100,000), whose dynamics should carry a robust signal of coupling.

We fit the semimechanistic absence–presence–absence model (Methods) to biweekly incidence data during the prevaccination era (1944–1964) in E&W, from the 872 smallest towns and cities (comprising 93% of all locations). The other 82 cities (with populations greater than 100,000) inform the analysis as additional donors of infection. Using the estimated model, we forward-simulate the timings of reintroductions and extinctions in each of the places. We compare the observed and simulated data on the basis of six key aspects of measles dynamics. Figure 2 shows that our estimated model accurately captures all these key aspects. We tested the overall inferential framework by assessing its performance on simulated data from a detailed metapopulation gravity model[9] (Supplementary Note 3).

Importance of core–satellite, LMP and random seeding. We calculate the relative risk of reintroduction between aggregate (predictable) interpopulation gravity-driven coupling (that is, core–satellite plus LMP) and unidentifiable random seeding (that is, any sources of reintroductions that are not captured explicitly by the gravitational components of our model structure) for each location (Fig. 1a,b). Note that, since reintroductions are defined to

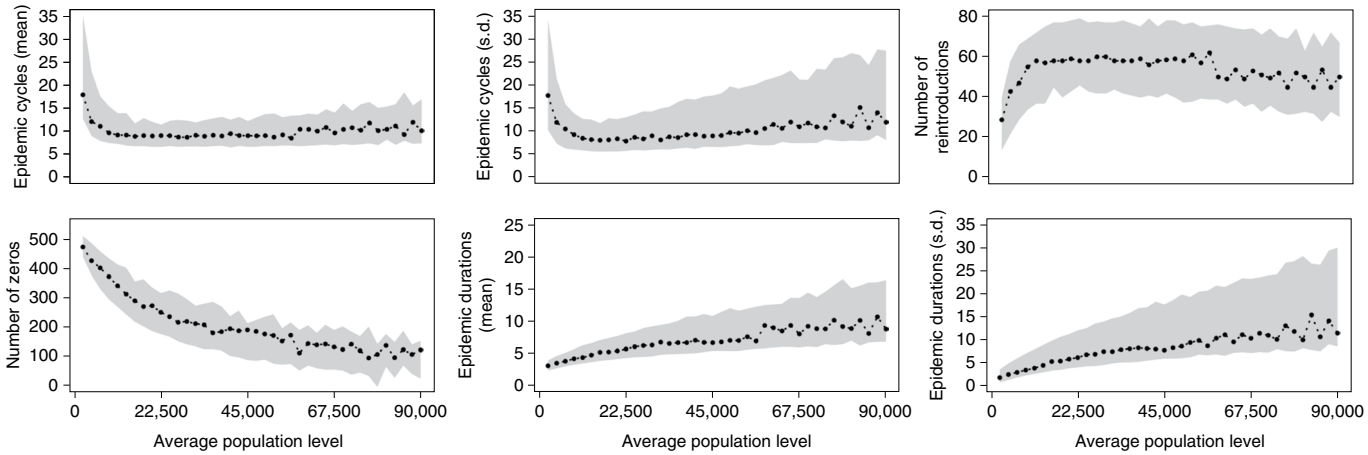

Fig. 2 | Fit of the absence–presence–absence model in the competing-risks framework from 1944 to 1964. Predictive distributions of the key aspects of measles dynamics: the number of reintroductions, the mean and standard deviation of epidemic cycles (that is, times, in the unit of biweek, between consecutive reintroductions), the number of biweeks with zero case reports, and the mean and standard deviation of epidemic durations (that is, times between reintroductions and extinctions; see also Fig. 1c). The grey bands represent 95% credible intervals (CIs), and the black dots correspond to the observed data. The locations (cities or towns) are binned equally into 40 levels according to their average population size (the *x* axis shows the upper limit of each interval).

occur only during local extinctions (Fig. 1c), local dynamics may not contribute substantially to any unidentifiable seeding in our context. Figure 3a shows the aggregate distribution across E&W for the entire prevaccination time series, suggesting that about 90% of the introductions can be accounted for by gravity coupling in this era. To get a more spatially resolved picture, we use local indicators of spatial association (LISA) (ref. [2]), capturing the relative importance of predictable versus random spread. The LISA analysis shows that random spread is considerably more important in peripheral areas (Cornwall, mid- and North Wales and East Anglia) than in the rest of E&W (Fig. 3b); isolated coastal areas feature especially in this group[22]. Despite the relative importance of erratic dynamics in the periphery compared with the rest of E&W, gravity-driven dynamics, absolutely speaking, remain dominant in these regions in the prevaccination era. Norwich and its environs, which became out of phase with the overall national trend during the 1950s, exhibiting even-year major epidemics, also appear as an outlier in terms of inferred metapopulation coupling.

The estimated model allows sampling of the source of infection for each reintroduction (Methods and Supplementary Note 2). We can therefore quantify the relative importance for each recipient community of each of the core cities, conditional on the sampled reintroductions of infections at each recipient community due to gravity coupling. Figure 3c shows the most influential donor city (among major core cities and other places) for each location (that is, the donor city that is responsible for the largest proportion of reintroductions). The prominent influence of London on the smaller towns around its periphery is broadly consistent with the hierarchical waves discussed in ref. [5]. Furthermore, Fig. 3c,d shows that, apart from the impact of a few core cities, LMP is an important driver in triggering reintroduction, with a median distance of transmission of 10.3 km. The average distance to the nearest neighbouring community in the data is 7.0 km (median, 5.3 km; interquartile range, 3.1 km–9.6 km). LMP thus extends out to the second-nearest neighbours, roughly speaking, in E&W's spatial network.

Gravity-driven versus geographically erratic spread over the history of vaccination. To investigate the changing roles of predictable gravity coupling (that is, core–satellite plus LMP) and unidentifiable seeding after the introduction of vaccination (Supplementary Fig. 1 and Fig. 1), we fit our model to five-year periods spanning the prevaccination era and the gradual increase in vaccination coverage during the 1970s and 1980s. For consistent spatial comparison through time, we use the post-1974 data aggregation (354 locations) to correct for changes in boundaries between the 1940s and 1990s (see Supplementary Note 1 for our method of aggregating the prevaccination data). To more explicitly measure the effect of unidentifiable sources relative to spatially predictable spread, we allow for different unidentifiable seeding parameters during different periods (Methods and Supplementary Note 2). Figure 4a depicts the location-wise distribution of risk due to spatially predictable and unidentifiable random seeding. It shows that the strength of gravity coupling diminished gradually with increasing vaccine coverage, while unidentifiable random seeding played an increasingly dominant role. Increased vaccination drove an increase in the CCS (Supplementary Fig. 1) and an overall decline in gravity-driven spread (Fig. 4b).

The increase in spatially erratic spread is also associated with a decay in both local and regional spatial synchrony in the vaccine era[5] (Fig. 4c). Before vaccination, the regional synchrony, measured by a non-parametric spatial correlation function (ranges between 0 and 1, with 1 representing complete spatial synchrony)[23], across E&W was 0.35, with a local above-average correlation of 0.65 that extended to a distance of 125 km. This collapsed to a region-wide synchrony of 0.03 in the 1990s with an above-average local synchrony of 0.06 (Fig. 4c). Importantly, the effective breakdown of the consumer-resource metapopulation could reinforce regional persistence through spatial transmission among asynchronous local epidemics; this could substantially hamper the likelihood of elimination, even at high vaccine uptake levels[24].

Discussion

Characterizing the drivers of measles outbreaks has important public health implications, in terms of optimizing vaccine deployment to achieve regional and then global elimination of infection. Recurrent measles outbreaks also illuminate fundamental questions regarding nonlinear population dynamics. Our analysis of the full urban hierarchy of measles outbreaks over 50 years in E&W sheds new light on regional dynamics and the impact of vaccination on these dynamics.

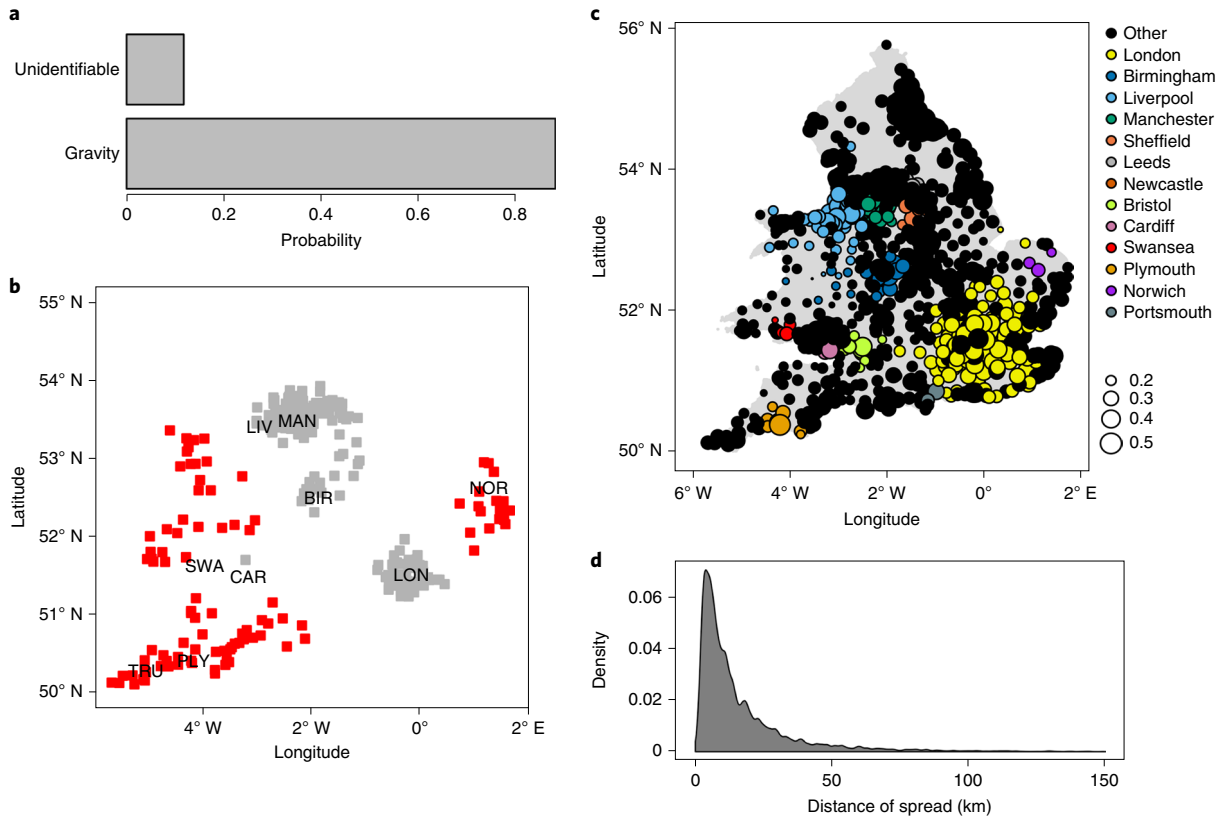

Fig. 3 | Prevaccination regional dynamics of measles, inferred from the absence–presence–absence model in a competing-risks framework. a, The crude global distribution of risk of reintroduction of infection due to spatially predictable (that is, core–satellite plus LMP) versus unidentifiable random seeding. **b**, Spatial hotspot analysis using LISA (refs. [2,34]) revealing the relative importance of unidentifiable erratic spread in peripheral areas. The red squares represent regions where the unidentifiable seeding is significantly important (at a nominal two-sided 5% level) relative to the average for E&W; the grey squares represent regions where gravity-driven patterns are significantly stronger (at a nominal two-sided 5% level). Geographical locations: NOR, Norwich; LON, London; MAN, Manchester; LIV, Liverpool; BIR, Birmingham; SWA, Swansea; CAR, Cardiff; PLY, Plymouth; TRU, Truro. **c**, Relative importance of core cities. The most influential city, which has the largest proportion of reintroductions (indicated by dot size) among all reintroductions in a recipient community owing to hierarchical gravity coupling, is shown. An 'other' city or town (a black dot) represents a place other than the considered core cities. **d**, The distribution of distance of spread from the most influential (non-core) cities (black dots) in **c**. The median distance of spread is 10.3 km (95% CI, 2.0, 72.5).

Inferring epidemiologically relevant local and regional movement (mainly of children for prevaccination measles) is a classic challenge in epidemiology. Here, we extend the existing rich body of work by developing a metapopulation framework that allows us to titrate the relative importance of different sources of reintroduction of infection, in the absence of explicit movement data. Rooted in transportation theory[14], the gravity model has been modified and widely applied in epidemiological and ecological studies for understanding the spatial dynamics of populations. The gravity framework for measles developed by Xia et al.[9] provided important insights, leveraged in subsequent gravity-themed models for measles[18] and other infections[15–17,19]. However, owing to its overparameterized formulation[18] (especially given the absence of explicit information on movement drivers; see Supplementary Note 2), direct and accurate quantification of spatial coupling and titration of the importance of different sources of reintroduction are difficult[18]. Building on previous work, we adapted the general concept of competing-risk frameworks[20] and derived a patch-level absence–presence–absence model, which allows us to accurately capture the signal of spatial coupling and explicitly quantify the importance of different sources for reintroductions across multiple eras of transmission.

Infective sparks of measles are conventionally assumed to spread from big cities like London to their nearby smaller conurbations, consistent with core–satellite dynamics. Our results give the most detailed quantification to date that LMP is also important in the spatial dissemination and regional persistence of infections[25]. LMP will be a critical challenge to tackle in designing control strategies for elimination. Our analysis also highlights that the vaccine-driven decorrelation of local epidemics is associated with a weakening of predictable gravity-driven spread and an increase in the dominance of erratic reintroductions from unidentifiable origins (consistent with genetic evidence that international importations of infections have become more influential in the vaccination era[26,27]). The transitions in spatial dynamics revealed in the unique E&W measles dataset illuminate how the regional and global elimination of infection is critically influenced by the interactions among changing local nonlinear clockworks, aggregate spatial transmission rates and the resulting emergent spatio-temporal dynamics. Understanding these interactions is increasingly urgent in the face of secular declines in vaccination and the re-establishment of measles endemism (seen post-1994 in E&W (ref. [28])).

As with any surveillance stream, our dataset is subject to a number of approximations (Supplementary Note 1); however, we believe that our overall results are robust to these (Supplementary Notes 1 and 2). A generic problem for projecting historical dynamics to the future are secular changes in system parameters. For measles, a particularly knotty example is behaviour change: the large prevaccination-era epidemics analysed here did not drive any major changes

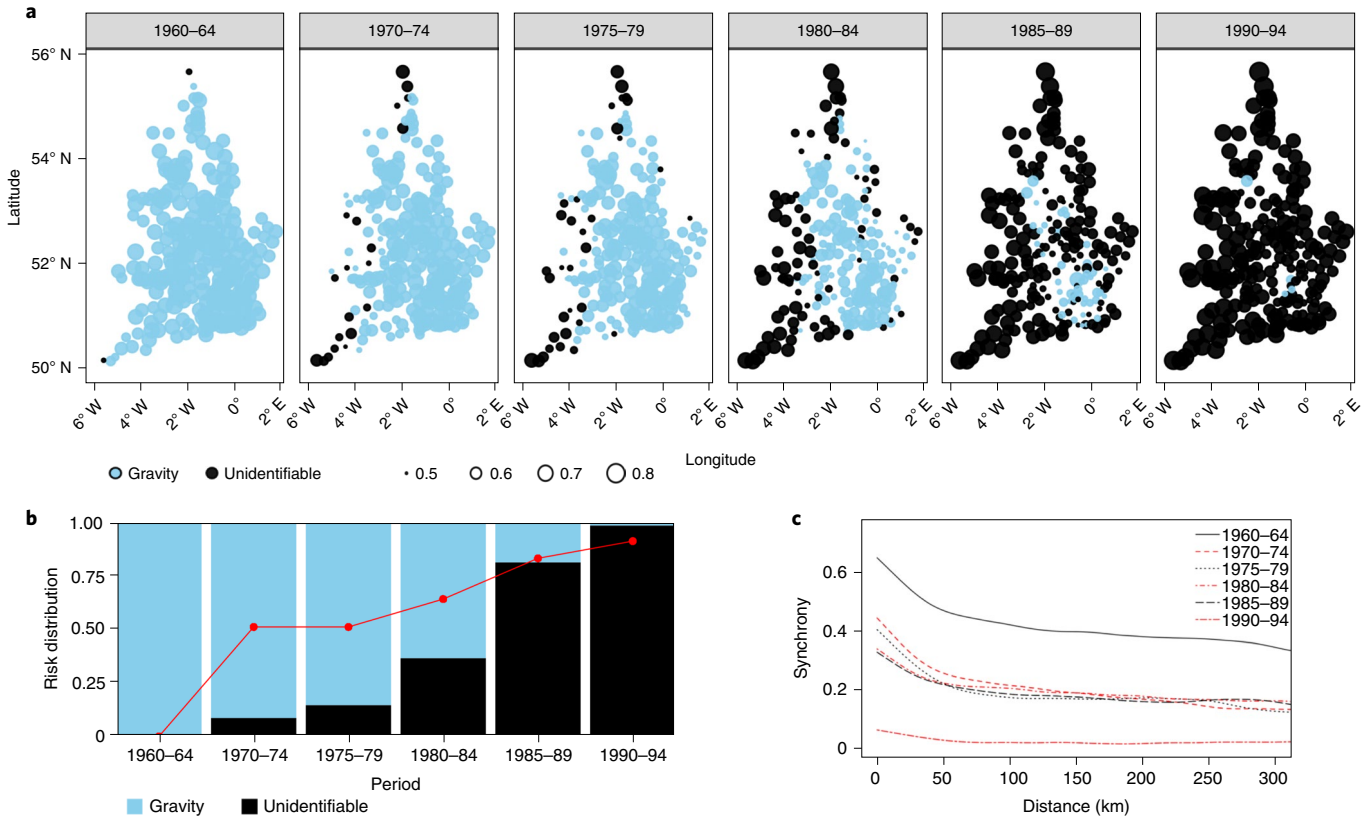

Fig. 4 | Impact of vaccination on the spatial spread of measles. a, Location-wise risk distribution for small places over the course of vaccine introduction and measles control in five-year windows. The size of a dot indicates the proportion of reintroductions that are due to the most impactful source of infection (gravity or unidentifiable seeding). Unidentifiable seeding became more widespread (that is, more black dots) and more prominent (that is, larger dot sizes) with increasing vaccination cover. **b**, Crude global risk distribution among unidentifiable versus gravity-driven seedings. The red line represents the average vaccination coverage. **c**, Although we find high local and regional synchrony[5] (as calculated by a non-parametric spatial correlation function[23]) of epidemics in the prevaccination era, asynchrony dominates during peak vaccination coverage as our model fails to identify the majority of importations. 1965–69 are not included here for the sake of clarity.

in behaviour for disease avoidance; in the present era, behaviour changes during epidemics (and hence the modulation of transmission) are more likely[29]. A powerful extension of historical analyses to allow for social and demographic variations in transmission would be the integration of epidemiological models with estimates of population susceptibility from periodic age-serological surveys[30].

Notwithstanding these complexities, there is considerable further scope to leverage historical datasets, such as presented here, to illuminate a range of both specific public health and general nonlinear population dynamic questions[31]. For example, the digitization of the full E&W Registrar General and OPCS (Office of Population and Census Survey) Weekly Reports back to 1855, of which the measles data presented here are a small part, would generate rich dynamical dividends on multiple important infections and questions.

Methods

Descriptive statistical methods. Standard methods (wavelets[5], non-parametric spatial correlation[23] and LISA (ref. [2])) are referenced in the text. All analyses were performed in R version 3.5.1.

Competing-risks framework with an absence–presence–absence model. The competing-risks framework aims to quantify spatial coupling processes beyond existing methods[9,18,21]. We do not model the local epidemic trajectories as considered in Xia et al.[9] (see Supplementary Note 3 for a simulation study with our framework). Our approach instead focuses on the local absence–presence–absence of infection via a susceptible–infected–susceptible–like patch-level model[32,33] where a spatial infection event (that is, a transition from absence to presence) corresponds to a reintroduction and the transition from presence to absence corresponds to a local extinction event (Fig. 1c). As reintroductions, defined to occur during local extinctions (Fig. 1c), are mostly due to the effect of (external) spatial coupling instead of (internal) seedings of local dynamics, our approach enables a direct quantification of spatial coupling. The transition from presence to absence is governed by a waiting time distribution that depends on introduction and susceptible recruitment rates[19]. Each location is classified as absent (and susceptible to reintroduction) in any given biweek if there were no cases of measles at the time or present if measles was reported (Supplementary Note 2). We embed our model within an explicit gravity network among all cities and towns. In particular, the force of reintroduction of infection p exerted on a particular town or city j by a city or town k at time t is

$$p(j,k,t) = \beta \times I_{k,t}^{\alpha_1} \times N_{j,t}^{\alpha_2} \times \frac{1}{d_{k,j}^{\rho}}$$

where $d_{k,j}$ is the distance between k and j, $I_{k,t}$ is the number of measles cases in k at t and $N_{j,t}$ is the population in j at t. We also consider unidentifiable background (random) sources of reintroduction of infection with rate τ, capturing any sources of reintroductions that are not captured explicitly by the gravitational components of our model structure. We formally capture the effect of local susceptibility by a parameter η (see Supplementary Note 2 for details). The model parameters are inferred using Bayesian inference with either non-informative or informative priors depending on data resolutions (Supplementary Note 2). Note that since reintroductions are defined to occur only during local extinctions (Fig. 1c), local dynamics may not contribute substantially to any unidentifiable seeding in our context. A link to the major code is included in the Supplementary Information.

Reporting Summary. Further information on research design is available in the Nature Research Reporting Summary linked to this article.

Data availability

The measles data are available at https://github.com/msylau/measles_competing_risks.

Code availability

The code is available at https://github.com/msylau/measles_competing_risks.

Received: 31 October 2019; Accepted: 27 March 2020;
Published online: 27 April 2020

References

1. Verguet, S. et al. Measles control in sub-Saharan Africa: South Africa as a case study. *Vaccine* **30**, 1594–1600 (2012).
2. Anselin, L. Local indicators of spatial association—LISA. *Geogr. Anal.* **27**, 93–115 (1995).
3. Sabbe, M. Measles resurgence in Belgium from January to mid-April 2011: a preliminary report. *Eurosurveillance* **16**, 19848 (2011).
4. Châtelet, I. P., du, Floret, D., Antona, D. & Lévy-Bruhl, D. Measles resurgence in France in 2008, a preliminary report. *Eurosurveillance* **14**, 19118 (2009).
5. Grenfell, B. T., Bjørnstad, O. N. & Kappey, J. Travelling waves and spatial hierarchies in measles epidemics. *Nature* **414**, 716–723 (2001).
6. Finkenstädt, B. F. & Grenfell, B. T. Time series modelling of childhood diseases: a dynamical systems approach. *J. R. Stat. Soc. Ser. C* **49**, 187–205 (2000).
7. King, A. A. & Schaffer, W. M. The geometry of a population cycle: a mechanistic model of snowshoe hare demography. *Ecology* **82**, 814–830 (2001).
8. Wilson, H. B. & Hassell, M. P. Host–parasitoid spatial models: the interplay of demographic stochasticity and dynamics. *Proc. R. Soc. Lond. B* **264**, 1189–1195 (1997).
9. Xia, Y., Bjørnstad, O. N. & Grenfell, B. T. Measles metapopulation dynamics: a gravity model for epidemiological coupling and dynamics. *Am. Nat.* **164**, 267–281 (2004).
10. Keeling, M. J. & Grenfell, B. T. Disease extinction and community size: modeling the persistence of measles. *Science* **275**, 65–67 (1997).
11. Bolker, B. M. & Grenfell, B. T. Impact of vaccination on the spatial correlation and persistence of measles dynamics. *Proc. Natl Acad. Sci. USA* **93**, 12648–12653 (1996).
12. Bak, P. *How Nature Works: The Science of Self-Organized Criticality* (Springer Science & Business Media, 2013).
13. Grenfell, B. & Harwood, J. (Meta)population dynamics of infectious diseases. *Trends Ecol. Evol.* **12**, 395–399 (1997).
14. Erlander, S. & Stewart, N. F. *The Gravity Model in Transportation Analysis: Theory and Extensions* (VSP, 1990).
15. Murray, G. D. & Cliff, A. D. A stochastic model for measles epidemics in a multi-region setting. *Trans. Inst. Br. Geogr.* **2**, 158–174 (1977).
16. Ferrari, M. J. et al. A gravity model for the spread of a pollinator-borne plant pathogen. *Am. Nat.* **168**, 294–303 (2006).
17. Viboud, C. et al. Synchrony, waves, and spatial hierarchies in the spread of influenza. *Science* **312**, 447–451 (2006).
18. Jandarov, R., Haran, M., Bjørnstad, O. & Grenfell, B. Emulating a gravity model to infer the spatiotemporal dynamics of an infectious disease. *J. R. Stat. Soc. Ser. C* **63**, 423–444 (2014).
19. Bjørnstad, O. N. & Grenfell, B. T. Hazards, spatial transmission and timing of outbreaks in epidemic metapopulations. *Environ. Ecol. Stat.* **15**, 265–277 (2007).
20. Birnbaum, Z. W. *On the Mathematics of Competing Risks* (US Dept. of Health, Education, and Welfare, Public Health Service, Office of the Assistant Secretary for Health, National Center for Health Statistics, 1979).
21. Bjørnstad, O. N., Finkenstädt, B. F. & Grenfell, B. T. Dynamics of measles epidemics: estimating scaling of transmission rates using a time series SIR model. *Ecol. Monogr.* **72**, 169–184 (2002).
22. Bharti, N., Xia, Y., Bjornstad, O. N. & Grenfell, B. T. Measles on the edge: coastal heterogeneities and infection dynamics. *PLoS ONE* **3**, e1941 (2008).
23. Bjørnstad, O. N. & Falck, W. Nonparametric spatial covariance functions: estimation and testing. *Environ. Ecol. Stat.* **8**, 53–70 (2001).
24. Graham, M. et al. Measles and the canonical path to elimination. *Science* **364**, 584–587 (2019).
25. Lloyd, A. L. & May, R. M. Spatial heterogeneity in epidemic models. *J. Theor. Biol.* **179**, 1–11 (1996).
26. Ramsay, M. E. et al. The elimination of indigenous measles transmission in England and Wales. *J. Infect. Dis.* **187**, S198–S207 (2003).
27. Jin, L., Brown, D. W., Ramsay, M. E., Rota, P. A. & Bellini, W. J. The diversity of measles virus in the United Kingdom, 1992–1995. *J. Gen. Virol.* **78**, 1287–1294 (1997).
28. Jansen, Va. A. et al. Measles outbreaks in a population with declining vaccine uptake. *Science* **301**, 804–804 (2003).
29. Gastañaduy, P. A. et al. Impact of public health responses during a measles outbreak in an Amish community in Ohio: modeling the dynamics of transmission. *Am. J. Epidemiol.* **187**, 2002–2010 (2018).
30. Metcalf, C. J. E. et al. Use of serological surveys to generate key insights into the changing global landscape of infectious disease. *Lancet* **388**, 728–730 (2016).
31. van Panhuis, W. G. et al. Contagious diseases in the United States from 1888 to the present. *N. Engl. J. Med.* **369**, 2152–2158 (2013).
32. Kermack, W. O. & McKendrick, A. G. A contribution to the mathematical theory of epidemics. *Proc. R. Soc. Lond. Math. Phys. Eng. Sci.* **115**, 700–721 (1927).
33. Keeling, M. J. & Rohani, P. *Modeling Infectious Diseases in Humans and Animals* (Princeton Univ. Press, 2008).
34. Bjornstad, O. N. *Package 'ncf': Spatial nonparametric covariance functions* v.1.1–7 (R Foundation for Statistical Computing, 2016); http://CRAN.R-project.org/package=ncf

Acknowledgements

We thank the RAPIDD Program of the US Department of Homeland Security and the Fogarty International Centre, National Institutes of Health (NIH). H.M.K. was also supported by the Eunice Kennedy Shriver National Institute of Child Health & Human Development of the NIH under award number P2CHD047879. A.D.B. was supported by a National Science Foundation Graduate Research Fellowship.

Author contributions

M.S.Y.L. designed the research. M.S.Y.L., A.D.B. and B.T.G. performed the research. M.S.Y.L. analysed the data. M.S.Y.L., A.D.B., H.M.K., Q.C., D.J.S., C.J.E.M., O.N.B. and B.T.G. wrote the paper.

Competing interests

The authors declare no competing interests.

Additional information

Supplementary information is available for this paper at https://doi.org/10.1038/s41559-020-1186-6.

Correspondence and requests for materials should be addressed to M.S.Y.L.

Reprints and permissions information is available at www.nature.com/reprints.

Publisher's note Springer Nature remains neutral with regard to jurisdictional claims in published maps and institutional affiliations.

nature research

Corresponding author(s): Max SY Lau

Last updated by author(s): Mar 25, 2020

Reporting Summary

Nature Research wishes to improve the reproducibility of the work that we publish. This form provides structure for consistency and transparency in reporting. For further information on Nature Research policies, see Authors & Referees and the Editorial Policy Checklist.

Statistics

For all statistical analyses, confirm that the following items are present in the figure legend, table legend, main text, or Methods section.

n/a	Confirmed
☐	☒ The exact sample size (*n*) for each experimental group/condition, given as a discrete number and unit of measurement
☐	☒ A statement on whether measurements were taken from distinct samples or whether the same sample was measured repeatedly
☐	☒ The statistical test(s) used AND whether they are one- or two-sided *Only common tests should be described solely by name; describe more complex techniques in the Methods section.*
☐	☒ A description of all covariates tested
☐	☒ A description of any assumptions or corrections, such as tests of normality and adjustment for multiple comparisons
☐	☒ A full description of the statistical parameters including central tendency (e.g. means) or other basic estimates (e.g. regression coefficient) AND variation (e.g. standard deviation) or associated estimates of uncertainty (e.g. confidence intervals)
☒	☐ For null hypothesis testing, the test statistic (e.g. *F*, *t*, *r*) with confidence intervals, effect sizes, degrees of freedom and *P* value noted *Give P values as exact values whenever suitable.*
☐	☒ For Bayesian analysis, information on the choice of priors and Markov chain Monte Carlo settings
☐	☒ For hierarchical and complex designs, identification of the appropriate level for tests and full reporting of outcomes
☒	☐ Estimates of effect sizes (e.g. Cohen's *d*, Pearson's *r*), indicating how they were calculated

Our web collection on statistics for biologists contains articles on many of the points above.

Software and code

Policy information about availability of computer code

Data collection	No software used.
Data analysis	Core statistical inference was performed using custom algorithm implemented in R (will be available soon on github). Other analyses (including data visualizations) were performed using open source R packages.

For manuscripts utilizing custom algorithms or software that are central to the research but not yet described in published literature, software must be made available to editors/reviewers. We strongly encourage code deposition in a community repository (e.g. GitHub). See the Nature Research guidelines for submitting code & software for further information.

Data

Policy information about availability of data

All manuscripts must include a data availability statement. This statement should provide the following information, where applicable:

- Accession codes, unique identifiers, or web links for publicly available datasets
- A list of figures that have associated raw data
- A description of any restrictions on data availability

All data generated or analysed during this study are included in this published article (and its supplementary information files).

Field-specific reporting

Please select the one below that is the best fit for your research. If you are not sure, read the appropriate sections before making your selection.

☐ Life sciences ☐ Behavioural & social sciences ☒ Ecological, evolutionary & environmental sciences

Ecological, evolutionary & environmental sciences study design

All studies must disclose on these points even when the disclosure is negative.

Study description	Modelling work to understand spatial transmission of measles and the effect of vaccination in the UK.
Research sample	*Describe the research sample (e.g. a group of tagged Passer domesticus, all Stenocereus thurberi within Organ Pipe Cactus National Monument), and provide a rationale for the sample choice. When relevant, describe the organism taxa, source, sex, age range and any manipulations. State what population the sample is meant to represent when applicable. For studies involving existing datasets, describe the data and its source.*
Sampling strategy	Weekly incidence data were recorded from each location listed in the Registrar General weekly reports.
Data collection	Registrar General weekly report data from January 1944 to December 1994 were double entered into spreadsheets by two people, blind to the others entries and then checked and cross-validated by one of us (DJS)
Timing and spatial scale	*Indicate the start and stop dates of data collection, noting the frequency and periodicity of sampling and providing a rationale for these choices. If there is a gap between collection periods, state the dates for each sample cohort. Specify the spatial scale from which the data are taken*
Data exclusions	No data were excluded.
Reproducibility	*Describe the measures taken to verify the reproducibility of experimental findings. For each experiment, note whether any attempts to repeat the experiment failed OR state that all attempts to repeat the experiment were successful.*
Randomization	*Describe how samples/organisms/participants were allocated into groups. If allocation was not random, describe how covariates were controlled. If this is not relevant to your study, explain why.*
Blinding	Blinding was used to cross-validate digitized data.

Did the study involve field work? ☐ Yes ☒ No

Reporting for specific materials, systems and methods

We require information from authors about some types of materials, experimental systems and methods used in many studies. Here, indicate whether each material, system or method listed is relevant to your study. If you are not sure if a list item applies to your research, read the appropriate section before selecting a response.

Materials & experimental systems

n/a	Involved in the study
☒	☐ Antibodies
☒	☐ Eukaryotic cell lines
☒	☐ Palaeontology
☒	☐ Animals and other organisms
☒	☐ Human research participants
☒	☐ Clinical data

Methods

n/a	Involved in the study
☒	☐ ChIP-seq
☒	☐ Flow cytometry
☒	☐ MRI-based neuroimaging